High-field magnetoexcitons in unstrained GaAs/Al$_x$Ga$_{1-x}$As quantum dots

Y. Sidor,* B. Partoens, and F. M. Peeters[†]

Departement Fysica, Universiteit Antwerpen (CGB), Groenenborgerlaan 171, B-2020 Antwerpen, Belgium

N. Schildermans, M. Hayne, and V. V. Moshchalkov

Pulsed Field Group, Laboratory of Solid State Physics and Magnetism, K.U. Leuven, Celestijnenlaan 200D, B-3001 Leuven, Belgium

A. Rastelli and O. G. Schmidt

Max-Planck-Institut für Festkörperforschung, Heisenbergstrasse 1, D-70569 Stuttgart, Germany

The magnetic field dependence of the excitonic states in unstrained GaAs/Al$_x$Ga$_{1-x}$As quantum dots is investigated theoretically and experimentally. The diamagnetic shift for the ground and the excited states are studied in magnetic fields of varying orientation. In the theoretical study, calculations are performed within the single band effective mass approximation, including band nonparabolicity, the full experimental three-dimensional dot shape and the electron-hole Coulomb interaction. These calculations are compared with the experimental results for both the ground and the excited states in fields up to 50 Tesla. Good agreement is found between theory and experiment.

PACS number(s): 73.21.La, 75.75.+a, 78.67.Hc

I. INTRODUCTION

Excitonic properties in quantum nanostructures have been intensively investigated over the past decade because of the high potential for applications and fundamental physics.[1–3] Among these nanostructures, quantum dots (QDs) are three-dimensional wells that can trap electrons and holes resulting in quantized energy levels. The density of states is δ functionlike, and the wave function of the particles is localized inside the dot. Therefore, excitons play an important role for the optical properties in such QDs. To explore these QD properties, optical spectroscopy experiments in the presence of an external magnetic field is a good probing tool.[4,5]

Semiconductor QDs can be grown by many methods, but in most cases are based on lithography and self-organization techniques. Self-assembled QDs formed through the Stranski-Krastanow growth mode, among the various 0D systems investigated so far, are the most well studied QDs. They can be fabricated with high uniformity and in a single layer (or in arrays of vertically aligned stacks). The optical properties of self-assembled QDs in the presence of an external magnetic field have been studied theoretically and experimentally by several groups. Early experimental work on InAs self-assembled QDs by Zhu *et al.*[6] and also by several other groups[7–10] observed the excitonic properties of different self-assembled dots in the presence of parallel and perpendicular magnetic fields. One should mention the interesting experimental and theoretical work done by Bayer *et al.*,[11] where self-assembled dots were investigated in magnetic fields of varying orientations. Theoretical approaches, based on a harmonic oscillator confinement potential and perturbation theory (see, for example, Ref. 12) have been presented in order to calculate the diamagnetic shift of the exciton ground state energy and to compare with the experimental data. Excited states in the dot were studied previously (see, for example, Refs. 13–16), both experimentally and theoretically by Raymond *et al.*[17] and in another experimental work

by Pulizzi *et al.*[18] In the work by Raymond *et al.* valence band mixing was included within the eight-band **k·p** model, coupled via the Bir-Pikus Hamiltonian to the strain of the dot calculated using classical elasticity theory. Very recently, experimental and theoretical results within the single band effective mass approximation including strain were presented in the absence of an external magnetic field, where the dot structure was taken directly from the experiment (possibly full 3D calculations). The ground state photoluminescence energy of the InAs/AlAs and InAs/GaAs QDs was calculated.[19]

GaAs/AlGaAs quantum dots cannot be created by Stranski-Krastanov growth because of the almost perfect match of lattice parameters. Nevertheless, this system offers several advantages compared to others: the grown material is ideally unstrained, and sharp interfaces with reduced intermixing can be obtained; they can be designed to emit light in the optimum spectral range of sensitive Si-based detectors. A new experimental method was presented recently to obtain GaAs/AlGaAs quantum dots via multistep (hierarchical) self-assembly. First a template of InAs/GaAs islands was created, which are "converted" into nanoholes on a GaAs surface by GaAs overgrowth followed by in situ etching. Self-assembled nanoholes are then transferred to an Al$_x$Ga$_{1-x}$As surface, filled with GaAs, and overgrown with Al$_y$Ga$_{1-y}$As ($x>y$). In this case the quantum dot morphology is given by the shape of the Al$_x$Ga$_{1-x}$As nanoholes.[20] This allows the electronic properties of the QDs to be calculated without the complication of uncertain composition and strain profiles.[20–22] The GaAs QDs are characterized by widely tunable emission energy, narrow inhomogeneous broadening (of the order of 8–20 meV depending on the growth parameters) and large separation between QD emission and continuum (up to ∼200 meV). Single-QD spectroscopy on such QDs show resolution-limited sharp lines,[20,23,24] single-photon emission up to 77 K and bright emission up to room temperature.[24]
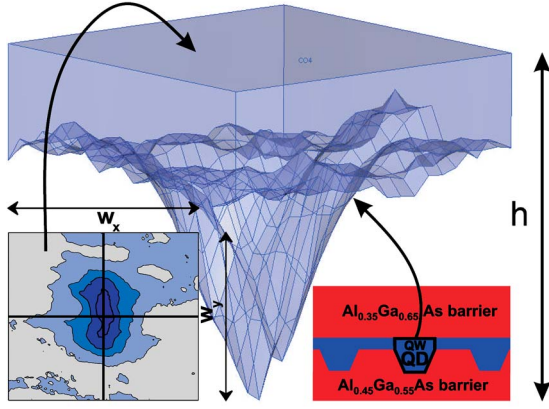
FIG. 1. (Color online) Geometry of the GaAs/Al$_x$Ga$_{1-x}$As QD, as measured by STM topography. The height $h=6.45$ nm and base widths along x and y directions $w_x=56$ nm and $w_y=72$ nm, respectively (x direction corresponds to the [1-10] crystal direction of GaAs). On the top of the dot a thin QW layer is deposited (for details see Refs. 20).

In this paper we focus our attention on the energy spectrum of single excitons in the presence of an applied magnetic field for such unstrained GaAs/Al$_x$Ga$_{1-x}$As QDs.[20] We perform calculations within the single band effective mass approximation but including band nonparabolicity in first order approximation. The real experimental shape of the dot with a quantum well on the top and asymmetrical AlGaAs barriers is considered. The calculations are based on a full 3D finite element scheme. We study the exciton energy shift for the ground and the excited states of the QD in magnetic fields up to 50 T of varying orientation.

The paper is organized in the following way. In Sec. II we briefly describe the method and the QD model used in our calculations. In Sec. III we discuss the Coulomb interaction energies and the wave function extensions of the particles in the presence of a magnetic field. Finally in Sec. IV, we present results of the influence of a magnetic field on the excitonic spectrum in GaAs/Al$_x$Ga$_{1-x}$As QDs, comparing theoretical and experimental data.

II. THEORETICAL FORMALISM AND MODEL

The geometry of the quantum dot was taken directly from scanning tunneling microscopy (STM) measurements. The profile of the 3D dot is illustrated in Fig. 1. On top of the GaAs dot-well system, an Al$_{0.35}$Ga$_{0.65}$As barrier was deposited, while on the bottom Al$_{0.45}$Ga$_{0.55}$As. Therefore, this structure is slightly nonsymmetric due to the different barriers. Figure 1 also shows the height (h) distribution in the 2D lateral profile of the dot with the base widths w_x and w_y. According to it, the dot is more elongated along the y direction, and the height distribution is not uniform with respect to the center of the xy plane.

The conduction and the valence bands are centered around the Γ valley of GaAs and Al$_x$Ga$_{1-x}$As. Within the single band effective-mass theory, in order to describe electron and hole states of the dots, we solve the Schrödinger equations

TABLE I. Material parameters used in the calculations: band gap E_g, electron mass m_e (Ref. 25), Luttinger parameters γ_1 and γ_2, nonparabolicity parameters α and β (Ref. 27), and dielectric constant ε (Ref. 28). For Al$_x$Ga$_{1-x}$As material parameters, the first-order interpolation formula is used: parameter(Al$_x$Ga$_{1-x}$As) = parameter(GaAs) ± x[parameter(GaAs)-parameter(AlAs)].

Parameter	GaAs	Al$_{0.35}$Ga$_{0.65}$As	Al$_{0.45}$Ga$_{0.55}$As
E_g (eV)	1.519	1.956	2.080
m_e (m_0)	0.067	0.096	0.104
γ_1	6.98	5.85	5.53
γ_2	2.06	1.63	1.50
α (eV^{-1})	0.64		
β (eV^{-1})	0.70		
ε	12.9	11.9	11.6

$$H\Psi(\mathbf{r}_e,\mathbf{r}_h) = E\Psi(\mathbf{r}_e,\mathbf{r}_h), \qquad (1)$$

with the Hamiltonian

$$H = H_e + H_h + U(\mathbf{r}_e - \mathbf{r}_h), \qquad (2)$$

where $H_{e(h)}$ denotes the single electron (hole) Hamiltonian, $U(\mathbf{r}_e-\mathbf{r}_h)$ is the Coulomb interaction between the electron and the hole

$$U(\mathbf{r}_e - \mathbf{r}_h) = -\frac{e^2}{\varepsilon|\mathbf{r}_e - \mathbf{r}_h|}, \qquad (3)$$

where e is the charge of the electron, and ε is the static dielectric constant taken as the value of GaAs, because of the very small difference of ε inside and outside the dot (see Table I).

In the presence of a magnetic field the momentum is replaced by the expression $\mathbf{p} \rightarrow \mathbf{p} - \frac{q}{c}\mathbf{A}$, so that the kinetic operator for the particles becomes

$$T = \left(\mathbf{p} - \frac{q}{c}\mathbf{A}\right)\frac{1}{2m^*}\left(\mathbf{p} - \frac{q}{c}\mathbf{A}\right), \qquad (4)$$

where q is the charge of the particle, m^* the spatial dependent mass of the particle, and $\mathbf{A}$ is the vector potential. Let us consider the case, when the magnetic field is applied along an arbitrary direction. We choose the symmetric gauge

$$\mathbf{A} = -\frac{1}{2}\mathbf{r} \times \mathbf{B}$$

$$= \frac{1}{2}[(B_y z - B_z y)\hat{x} + (B_z x - B_x z)\hat{y} + (B_x y - B_y x)\hat{z}],$$

where B_x, B_y, and B_z are the components of the magnetic field along the x, y, and z directions, respectively, given by

$$B = (B_x, B_y, B_z) = B[\cos(\varphi)\sin(\theta), \sin(\varphi)\sin(\theta), \cos(\theta)],$$
$$(5)$$

where $(0 \leqslant \theta \leqslant \pi, \ 0 \leqslant \varphi \leqslant 2\pi)$. Inclusion of the magnetic field leads to fifteen additional diamagnetic terms in the kinetic term, in addition to $\mathbf{p}[1/(2m^*)]\mathbf{p}$. From them, twelve are linear with respect to B_i, r_i, and ∇_i ($i=x$, y, and z; here

and further we will use $r_x = x$, $r_y = y$, and $r_z = z$), and three other are quadratic

$$C \sum_{i(j,k)=x}^{y,z} \frac{(B_i r_j - B_j r_i)^2}{m_k^*}, \qquad (6)$$

where the constant $C = q^2/(8c^2)$, and m_k^* are the position dependent components of the effective mass tensor.

In the QD structure the subband energy due to the z-confinement is typically of the order of 100 meV. Therefore, the anisotropy and the corrections due to the conduction band nonparabolicity are important.[26] The electron Hamiltonian is

$$H_e(r_e) = -\nabla_{xe} \frac{\hbar^2}{2m_{\|e}^*(\mathbf{r}_e)} \nabla_{xe} - \nabla_{ye} \frac{\hbar^2}{2m_{\|e}^*(\mathbf{r}_e)} \nabla_{ye}$$
$$- \nabla_{ze} \frac{\hbar^2}{2m_{\perp e}^*(\mathbf{r}_e)} \nabla_{ze} + V_e(\mathbf{r}_e) + V_{eB}(\mathbf{r}_e), \qquad (7)$$

where $V_e(r_e)$ is the conduction band offset and we took the asymmetry of the AlGaAs barriers and the geometry of the dot into account (see Fig. 1). $V_{eB}(r_e)$ denotes the aforementioned electron diamagnetic terms $m_{\|e}^*$ and $m_{\perp e}^*$ are the perpendicular and parallel effective masses of the electron, which we obtain from the first order nonparabolicity approximation[27]

$$m_{\perp e}^* = m_e^*(1 + \alpha E), \qquad (8a)$$

$$m_{\|e}^* = m_e^*[1 + (2\alpha + \beta)E], \qquad (8b)$$

where m_e^* is the bulk electron masses of the material, α and β are the nonparabolicity parameters (see Table I), and E is the ground state energy of the electron obtained by solving the single particle Schrödinger equation using the bulk masses of the electron. The parallel mass determines the electron energy in the xy plane, and the perpendicular mass determines the quantization energy of the electrons in the z direction.

We consider both the heavy-hole (hh) and the light-hole (lh) states in our calculation. The strain is not included because the QD structure is unstained due to the experimental growth conditions.[20] The single particle Hamiltonian for both holes (h) is

$$H_h(r_h) = -\nabla_{xh} \frac{\hbar^2}{2m_h^*(\mathbf{r}_h)} \nabla_{xh} - \nabla_{yh} \frac{\hbar^2}{2m_h^*(\mathbf{r}_h)} \nabla_{yh}$$
$$- \nabla_{zh} \frac{\hbar^2}{2m_h^*(\mathbf{r}_h)} \nabla_{zh} + V_h(\mathbf{r}_h) + V_{hB}(\mathbf{r}_h), \qquad (9)$$

where m_h^* is the effective masses of the hole, $V_h(r_h)$ is the valence band confinement offset of the hole, $V_{hB}(r_h)$ denotes the hole diamagnetic terms. Note that this single particle Hamiltonian is not just the diagonal part of the four-band $\mathbf{k} \cdot \mathbf{p}$ Hamiltonian. The mass in each direction is the same and corresponds to the curvature of the hole bands around the Γ point, i.e., for the heavy-hole and the light-hole, respectively,

$$\frac{m_0}{m_{hh}^*} = \gamma_1 - 2\gamma_2, \qquad (10a)$$

$$\frac{m_0}{m_{lh}^*} = \gamma_1 + 2\gamma_2, \qquad (10b)$$

where γ_1 and γ_2 are Luttinger parameters (see Table I), and m_0 is the vacuum electron mass.

To include the Coulomb interaction between the electron and the hole in the QD, we calculate the Hartree potential $\varphi(r)$ by solving the 3D Poisson equation

$$\varepsilon \nabla^2 \varphi(\mathbf{r}) = -4\pi\rho(\mathbf{r}), \qquad (11)$$

where $\rho(\mathbf{r})$ is the particle density, previously calculated from Eq. (1). The potential $\varphi(\mathbf{r})$ is the one felt by the hole, i.e., in mathematical terms it means $\varphi(\mathbf{r}_h) \approx \int d\mathbf{r}_e \rho(r_e)/|\mathbf{r}_e - \mathbf{r}_h|$. To solve the Poisson equation, often one uses zero as the boundary condition, which is a good approximation when a large enough grid is used. The regular asymptotic boundary condition to the Poisson equation is proportional to $1/r$. Note, because the dot profile is not symmetric, consequently the density of the electron is not symmetric, and therefore the exact asymptotic boundary condition for the last equation becomes

$$\varphi(\mathbf{r}_e) = \frac{q}{\varepsilon|\mathbf{r}_e - \mathbf{r}_{0e}|}, \qquad (12)$$

where $\mathbf{r}_{0e} = \int \mathbf{r}_e \rho(\mathbf{r}_e) d\mathbf{r}_e$ is the average value of the coordinates of the electron, and q is the electron charge. The Coulomb energy, which accounts for the interaction between the electron-hole pair, is obtained by performing 3D integration over the hole coordinates

$$E_C = \int \varphi(\mathbf{r}_h) \rho(\mathbf{r}_h) d\mathbf{r}_h, \qquad (13)$$

where $\rho(r_h)$ is the hole density. Note, that by solving the Poisson equation we circumvent the direct 6D integration over electron and hole space, and we avoid the $1/r$ singularity problem for $r \to 0$.

The full 3D calculations with the real shape of the dot in the presence of the magnetic field, as well as the Poisson equation are performed using the finite element method on a variable size grid. The input parameters used in the simulations are presented in Table I. Most of the parameters have been taken from Ref. 29, otherwise indicated.

III. EXTENT OF THE PARTICLES AND THE COULOMB INTERACTION ENERGIES

In this section we discuss the electron-hole interaction and the wave function extensions of the particles in the presence of a magnetic field. One should stress that there are no fitting parameters in all our calculations.

The mass of the heavy-hole inside the dot, is equal to $0.35m_0$, and is four times larger than the mass of the light-hole $0.09m_0$ [see Eqs. (10a) and (10b) and Table I]. As a result, the wave function radii in the xy plane of the heavy-hole for zero magnetic field **B** are smaller than for the light-hole, as can be seen from Fig. 2. However, one can notice that the electron extent is smaller than for the light-hole. The reason is that, although the electron mass is a bit lighter than
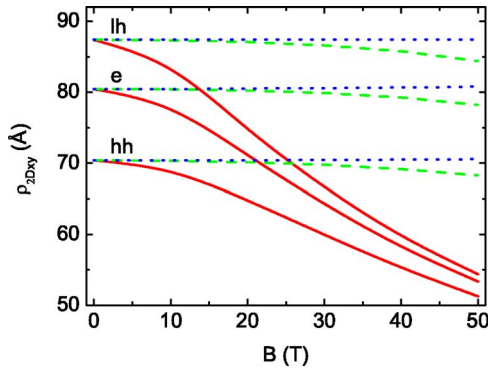
FIG. 2. (Color online) The extent of the electron (e), the heavy-hole (hh), and the light-hole (lh) in the xy plane, as a function of the magnetic field **B** for GaAs/Al$_x$Ga$_{1-x}$As QD. The dashed (green), dotted (blue), and full (red) curves correspond to the radii, when the magnetic field is applied along the x, y, and z direction, respectively.

the one of the light-hole, the conduction band offset is roughly 1.5 times larger than the offset for the light-hole. Let us comment on the behavior of the particle radii in the case when the magnetic field is applied along the z direction. The magnetic field influences the particle motion in the plane perpendicular to the applied direction. When the magnetic field is applied along the z direction (influence on the xy plane), the 2D radii in the xy plane are strongly squeezed for all particles (see full curves in Fig. 2), and it leads to a decrease of at least 30% (even more for the light-hole). This large change is due to the flatness of the dot, with a lateral dimension about 10 times larger than its height. This is the reason why the magnetic field applied along the x and y directions has a less pronounced effect on the electron and holes 2D extension (see dashed and dotted curves in Fig. 2, respectively). The dot is slightly larger in the y direction which explains the small difference between the dashed and dotted curves in Fig. 2.

Radii along the z direction are significantly smaller than those in the plane, as depicted in Fig. 3. The electron radius is smaller than the one for the light-hole, because of the difference of conduction and valence band offsets. When the magnetic field is applied along the z direction, the wave function is squeezed in the plane of the dot, as was already
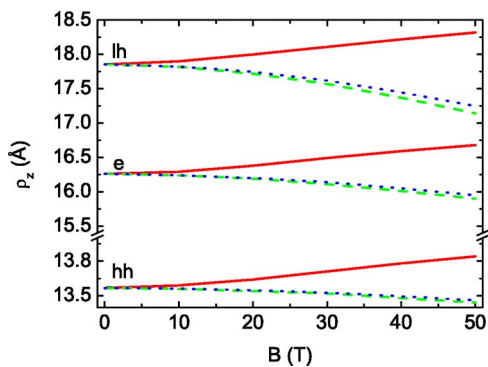

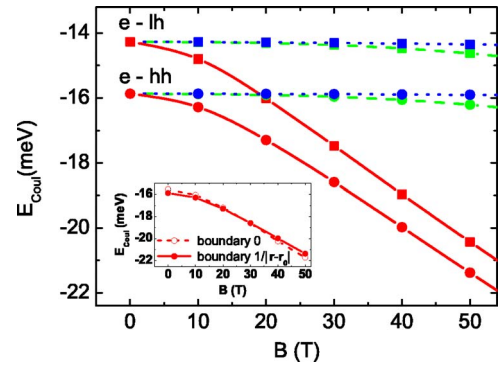FIG. 3. (Color online) The same as Fig. 2 but now in the z direction.

FIG. 4. (Color online) The electron-hole Coulomb interaction energy as a function of magnetic field for GaAs/Al$_x$Ga$_{1-x}$As QD. The dashed (green), dotted (blue), and full (red) curves with the circles correspond to the heavy-hole-electron Coulomb energies, for the magnetic field applied along the x, y, and z direction, respectively. The curves with the squares represent the light-hole-electron Coulomb interaction energies. The inset shows the Coulomb energy, as a function of magnetic field applied along the z direction. The dashed (full) curves with the open (closed) circles correspond to the two different boundary conditions of the Poisson equation.

observed, but at the same time it will become elongated in the z direction (full curves in Fig. 3), because the total particle probability is a constant. This is similar to squeezing a balloon in two directions. In the case of the magnetic field applied along the x and y directions (dashed and dotted curves in Fig. 3, respectively), the particle radii slightly decrease with increasing magnetic field due to the squeezing of the wave function in, respectively, the yz and xz plane.

The dependence of the electron-hole Coulomb interaction on the external magnetic field is shown in Fig. 4. As was mentioned in Sec. II, one can use different boundary conditions for the Poisson equation. In the inset of Fig. 4 we show that by using the boundary condition described by Eq. (12) and the one with zero boundary conditions may influence the Coulomb interaction energy slightly. The absolute value of the Coulomb interaction is inversely proportional to the relative distance between the electron and the hole. The radii for all the particles in the xy plane are much larger than that along the z direction. Therefore, the interaction between the electron and the hole is predominantly determined by the behavior of the particle radii in the xy plane (compare Figs. 2, 3, and 4), i.e., for the magnetic field applied along the z direction an increase of the absolute value of the Coulomb energy for both electron-heavy-hole and electron-light-hole pairs is observed. Only a very small increase with applied magnetic field along the plane of the dot (see the dashed and dotted curves with circles and squares in Fig. 4) is seen.

IV. MAGNETOEXCITON TRANSITIONS AND COMPARISON BETWEEN THEORY AND EXPERIMENT

In this section we investigate the exciton diamagnetic shift of the dot. We perform our simulations for both heavy- and light-hole states and compare them with the experimental data. The experimental data are obtained by photolumi-
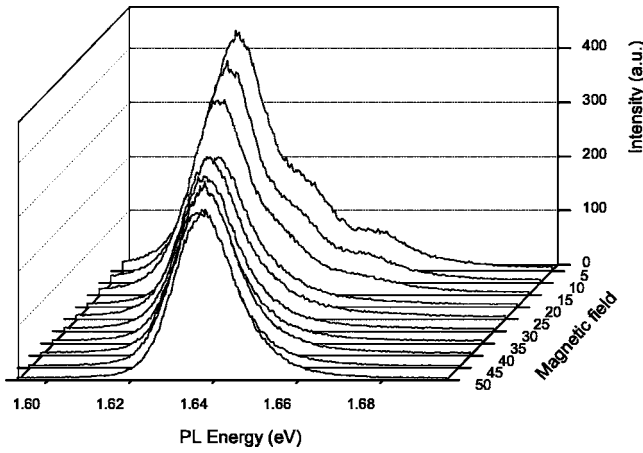
FIG. 5. Photoluminescence spectra as a function of magnetic field applied parallel to the z direction. The peak positions of ground and excited states are obtained by Gaussian fits.

nescence measurements in pulsed magnetic fields up to 50 T (see Fig. 5). The experiments were carried out in a He[4]-bath cryostat at 4.2 K, using an argon-ion laser at a wavelength of 514 nm to excite the electrons. The photoluminescence (PL) was analyzed by a spectrometer and an intensified charged-coupled-device detector, using an integration time of 0.5 ms. The peak positions of the PL spectrum are obtained by Gaussian fits to the experimental spectra. The measured PL ground state energy versus field dependence can be fitted with an excitonic model, using three parameters: the zero field PL energy, exciton wave function radius and the exciton mass. The exciton radius in the xy plane obtained with the fitting procedure from the experimental data of 7.6 nm is in good agreement with the calculated electron radius as described in the previous section. A detailed description of the experimental setup and analyzing method can be found in Ref. 5.

In Fig. 6 we examine the diamagnetic shift of the ground state exciton energy, with and without taking into account the Coulomb interaction, when the magnetic field is applied
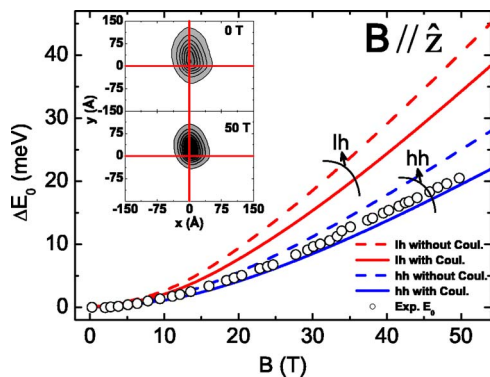

FIG. 6. (Color online) The diamagnetic shift of the exciton ground state energy, as a function of a magnetic field along the z direction for GaAs/Al$_x$Ga$_{1-x}$As QD. The full and dashed curves correspond to the heavy-hole and the light-hole excitons with and without taking into account the Coulomb interaction. The inset shows the contour plot of the electron density at magnetic field 0 and 50 T.
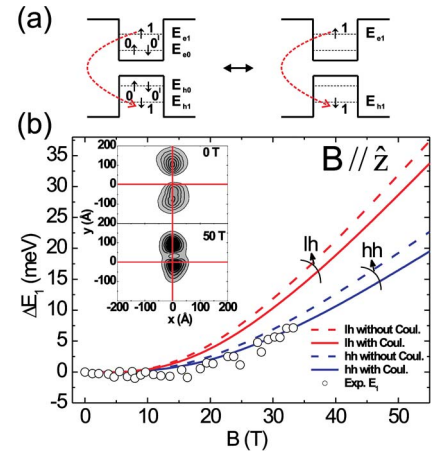

FIG. 7. (Color online) (a) Schematic of the excitonic levels for the first excited state. (b) The diamagnetic shift of the first excited exciton state, as a function of magnetic field applied along the z direction for GaAs/Al$_x$Ga$_{1-x}$As QD. The full and dashed curves correspond to the heavy-hole and the light-hole excitons with and without taking into account the Coulomb interaction. The inset shows the contour plot of the electron density of the first excited state at magnetic field 0 and 50 T.

along the z direction. From Fig. 6 we can immediately notice the importance of including the Coulomb interaction energy (compare full and dashed curves). The resulting diamagnetic shift is inversely proportional to the reduced mass of the electron and hole. The heavy-hole mass is four times larger in the xy plane of the dot than the lighthole. Consequently, the resulting heavy-hole diamagnetic shift is smaller than the light-hole diamagnetic shift, when the magnetic field is applied along the growth direction ($\mathbf{B}//\hat{z}$). Up to 35 T the calculated diamagnetic shift energies for the heavy-hole states are in very good agreement with the experimental data. At 50 T the disagreement between theory and experiment is less than 1 meV. If we exclude the nonparabolicity of the electron mass the disagreement between the theoretical heavy-hole exciton and the experiment at 50 T is 3 meV. In the inset of Fig. 6 we show a contour plot of the electron density which illustrates the asymmetry of the electron density regarding the xy center. The zero magnetic field PL energies for the heavy-hole state is $E_{PLhh}=1614$ meV, which compares to the experimental PL energy $E_{PLexp}=1620$ meV, while for the light-hole we found $E_{PLlh}=1652$ meV. We neglected the Zeeman effect in our calculations, since even at the highest magnetic field it gives only a small contribution. Taking the g_{ex} factor for the exciton equal to 0.51,[30] the Zeeman splitting energy between the states with the spin up and down is only $g_{ex}\mu_B B \approx 1.5$ meV at 50 T, where μ_B is the Bohr magneton.

Figure 7(b) shows the exciton diamagnetic shift of the first excited state in the presence of a magnetic field applied along the z direction. In the experiment, the PL intensity of the first, and particularly the second, excited states is quenched with magnetic field, such that experimental data is only available up to 35 and 10 T for the first and second excited states, respectively. Our calculations demonstrate that there is an enhancement of the electron-hole wave-function

overlap with magnetic field (not shown). Thus, since the intensity of the ground state PL also becomes slightly less intense with magnetic field, this implies that electron-hole pair capture by the dots is suppressed at high fields. Theoretically, we investigate both heavy- and light-hole exciton states with and without taking into account the electron-hole interaction. In the whole magnetic field region of available experimental data, up to 35 T, we again see a quantitative agreement with the heavy-hole diamagnetic shift when including the Coulomb interaction. Comparing the PL energies, the heavy-hole state is also closer to the experimental PL energy E_{PLexp}=1638 meV, E_{PLhh}=1630 meV, and E_{PLlh} =1673 meV. Furthermore, if we compare the heavy-hole PL energy difference between the first excited state and the ground state $\Delta E_{\mathrm{PLhh}(1,0)}$=16 meV with the experimental values $\Delta E_{\mathrm{PLexp.}(1,0)}$=18 meV, it gives further support to our claim that the heavy-hole exciton is the ground state. In the inset of Fig. 7(b) we illustrate the electron densities of the first excited state for a magnetic field of 0 and 50 T.

The exciton energy was calculated, as $E_{\mathrm{ex},i}=E_{e,i}+E_{h,i}-E_{C(ei,hi)}$, where i=0 refers to the ground state, i=1 to the first excited state, and so on; and $E_{C(ei,hi)}$ is the Coulomb interaction between the electron-hole (heavy and light-holes) pair in the ith state. Knowing this exciton energy, we calculate the exciton diamagnetic shift energy ΔE_i. One should stress, that we assume the recombination between electron and hole of the same quantum state, namely, electron and hole are either both in the ground state or in the first or second excited state, which is experimentally and theoretically justified[14,15,17,18] on the basis of selection rules. Moreover, we consider the possibility of multiexcitonic transitions. Let us compare two situations: (1) each particle is in the first excited state [see the right graph in Fig. 7(a)], which corresponds to the first excited state of the exciton, and (2) the two identical particles (electron or hole) with spin up and down are in the ground state and one in the first excited state [see the left graph in Fig. 7(a)], which corresponds to the ground state of the three exciton line. In the first case we have for the diamagnetic shift for the excited exciton the terms $\Delta E_{e1}+\Delta E_{h1}-E_{C(e1,h1)}$. In the second case, instead of $-E_{C(e1,h,1)}$ appears $2E_{C(e0,e1)}+2E_{C(h0,h1)}-2E_{C(e0,h1)}-2E_{C(e1,h0)}-E_{C(e1,h1)}$. Here $E_{C(e0,e1)}$ is the electron correlation energy of the ground and first excited states, $E_{C(h0,h1)}$ is the hole correlation energy, and the rest are the Coulomb interaction energies between the ground and first excited states of the particles. We computed the aforementioned correlation and Coulomb interaction energies for the heavy-hole state, as an example, in order to estimate the distinction. However, we found that the difference between the first excited state of the single exciton transition and the ground state of the three exciton-line transition is very small. It is less than 1 meV at zero magnetic field, and about 1 meV at 50 T. The same situation arises if we compare the ground state of the exciton (electron and hole are in the ground state) and the ground state of the two exciton-line (two electrons and holes are in the ground state). The difference is also less than 1 meV at magnetic field 0 and 50 T.
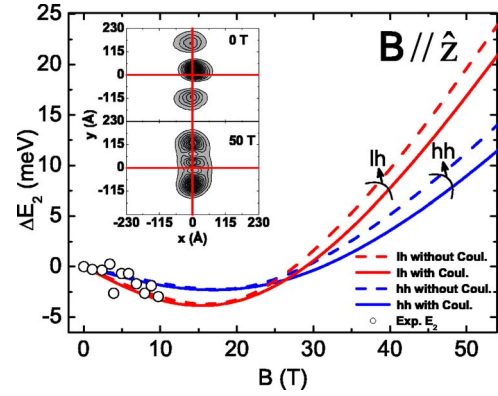

FIG. 8. (Color online) The same as Fig. 6 but now for the second excited state.

Comparison between our theoretical simulations for the exciton diamagnetic shift of the second excited state and available experimental data are shown in Fig. 8. Since there are only experimental data for magnetic fields up to 10 T, it is difficult to judge, whether heavy- or light-hole exciton states are in good agreement with the experiment (see curves for the heavy-hole and the light-hole with and without Coulomb interaction). Comparing the PL energies, the heavy-hole state is closer to the experimental PL energy E_{PLexp}=1650 meV, E_{PLhh}=1644 meV, and E_{PLlh} =1692 meV. When we compare the heavy-hole PL energy difference between the second excited state and the first excited state with the experimental data, we found that $\Delta E_{\mathrm{PLhh}(2,1)}$=14 meV and $\Delta E_{\mathrm{PLexp}(2,1)}$=12 meV, which is another justification that the experimental results correspond with heavy-hole excitons. However, for both hole states we observe a negative diamagnetic shift, with increasing magnetic field for B<15 T, which agrees with the experimental data (see open circles). Let us remember, that including the magnetic field causes an extra parabolic confinement, as described by Eq. (7). The well known Fock-Darwin spectrum at small values of the magnetic field, where the 2D harmonic oscillator is considered, shows a small negative dependence of the first excited state energy, which is more pronounced after the crossing of the second and third excited state energies. However, the negative excitonic diamagnetic shift is seen for the second excited state both in the theoretical and experimental results (compare Figs. 7 and 8). In the inset of Fig. 8 the change of the electron density for the second excited state for the magnetic fields of 0 and 50 T is plotted.

We also investigate the exciton diamagnetic shift of the QD in the presence of a magnetic field perpendicular to the z direction ($\mathbf{B} \perp \hat{z}$). As an example we consider the exciton diamagnetic shift, when the magnetic field is applied along the x, y direction, and directed 45° between the xy direction (see Fig. 9). The Coulomb interaction energy, as was already discussed in Fig. 4, has a negligible effect on the magnetic field dependence. For magnetic fields up to 40 T the experimental points are between the heavy- and light-hole curves, and for high magnetic field a good agreement between the experimental points and the theoretical heavy-hole diamagnetic shift is obtained. Within the single band model it is not possible to take into account the coupling between the
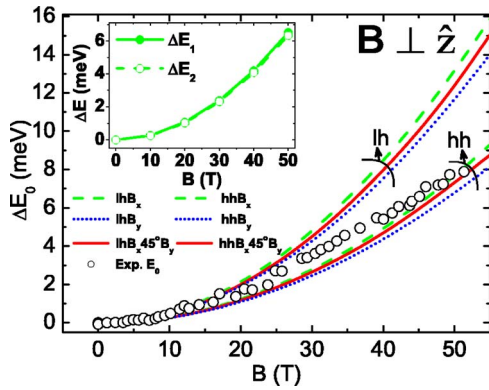
FIG. 9. (Color online) The diamagnetic shift of the exciton ground state, as a function of magnetic field. The dashed (green) and dotted (blue) curves correspond to the heavy-hole and the light-hole excitons, when the magnetic field is applied along the x and y direction, respectively. The full (red) curves correspond to the case, when the magnetic field is applied along 45° between the xy direction. The inset shows the heavy-hole exciton diamagnetic shift of the first (E_1) and second (E_2) excited state, when the magnetic field is applied along the x direction.

heavy-hole and the light-hole, which is the most likely reason for the discrepancy at magnetic fields up to 40 T. Note, that there is a large distinction in the diamagnetic field between heavy- and light-hole states. The difference for the magnetic field applied along the x, y direction, or 45° between xy direction is small. The inset of Fig. 9 shows the heavy-hole exciton diamagnetic shifts (the light-hole excitons have the same behavior) for the two lowest excited states. The dot confinement is more important than the magnetic confinement at small magnetic field. Hence, we do not observe a negative diamagnetic shift behavior for both excited states.

V. CONCLUSIONS

In summary, the excitonic properties in the presence of a magnetic field in unstrained $GaAs/Al_xGa_{1-x}As$ QDs were investigated theoretically and experimentally. In our 3D calculations, within the single band effective mass approximation, we include the effect of band nonparabolicity of the conduction band, the real shape of the QD with the thin well layer on top and asymmetrical barrier materials, as well as heavy- and light-hole states. By solving the Poisson equation with the correct boundary conditions, the Coulomb interaction energy between electron and hole was calculated.

The magnetic field dependence of the electron-hole Coulomb interaction energy, when the magnetic field is applied along x, y, and z direction, follows closely the dependencies of the particle radii (i.e., size) in the xy plane of the dot. Radii along the z direction are significantly smaller due to the flatness of the dot, and with increasing magnetic field along the z direction the particles wave function radii become elongated in the z direction.

The diamagnetic shift for the exciton ground state and the two first excited states in the presence of a magnetic field applied along x, y, and z direction in the QD are calculated. A good agreement between the experimental results and the calculated heavy-hole exciton is found. By comparing the PL energies, the heavy-hole state is found to be the ground state, and its value is close to the experimental data.

*Electronic address: yosyp.sidor@ua.ac.be

†Electronic address: francois.peeters@ua.ac.be

[1] See, for example, L. Esaki and R. Tsu, IBM J. Res. Dev. **14**, 61 (1970).

[2] See, for example, Y. Arakawa and H. Sakaki, Appl. Phys. Lett. **40**, 939 (1982).

[3] See, for example, M. Grundmann, D. Bimberg, and N. N. Ledentsov, *Quantum Dot Heterostructures* (Wiley, New York, 1998).

[4] S. Smith, A. Mascarenhas, and J. M. Olson, Phys. Rev. B **68**, 153202 (2003).

[5] M. Hayne, J. Maes, S. Bersier, M. Henini, L. Müller-Kirsch, R. Heitz, D. Bimberg, and V. V. Moshchalkov, Physica B **346-347**, 421 (2004).

[6] H. J. Zhu, M. Ramsteiner, K. H. Ploog, R. Zhang, R. Tsui, K. Shiralagi, and H. Goronkin, Phys. Rev. B **62**, R16314 (2000).

[7] M. Hayne, R. Provoost, M. K. Zundel, Y. M. Manz, K. Eberl, and V. V. Moshchalkov, Phys. Rev. B **62**, 10324 (2000).

[8] Mitsuru Sugisaki, Hong-Wen Ren, Selvakumar V. Nair, Kenichi Nishi, and Yasuaki Masumoto, Phys. Rev. B **66**, 235309 (2002).

[9] S. Smith, A. Mascarenhas, and J. M. Olson, Phys. Rev. B **68**, 153202 (2003).

[10] M. Hayne, O. Razinkova, S. Bersier, R. Heitz, L. Müller-Kirsch, M. Geller, D. Bimberg, and V. V. Moshchalkov, Phys. Rev. B **70**, 081302(R) (2004).

[11] M. Bayer, O. Stern, A. Kuther, and A. Forchel, Phys. Rev. B **61**, 7273 (2000).

[12] D. Reuter, P. Kailuweit, A. D. Wieck, U. Zeitler, O. Wibbelhoff, C. Meier, A. Lorke, and J. C. Maan, Phys. Rev. Lett. **94**, 026808 (2005).

[13] O. Stier, M. Grundmann, and D. Bimberg, Phys. Rev. B **59**, 5688 (1999).

[14] S. Raymond, X. Guo, J. L. Merz, and S. Fafard, Phys. Rev. B **59**, 7624 (1999).

[15] M. Bayer, O. Stern, P. Hawrylak, S. Fafard, and A. Forchel, Nature (London) **405**, 923 (2000).

[16] K. L. Janssens, F. M. Peeters, and V. A. Schweigert, Phys. Rev. B **63**, 205311 (2001).

[17] S. Raymond, S. Studenikin, A. Sachrajda, Z. Wasilewski, S. J. Cheng, W. Sheng, P. Hawrylak, A. Babinski, M. Potemski, G. Ortner, and M. Bayer, Phys. Rev. Lett. **92**, 187402 (2004).

[18] F. Pulizzi, D. Walker, A. Patané, L. Eaves, M. Henini, D. Granados, J. M. Garcia, V. V. Rudenkov, P. C. M. Christianen, J. C. Maan, P. Offermans, P. M. Koenraad, and G. Hill, Phys. Rev. B **72**, 085309 (2005).

[19] P. Offermans, P. M. Koenraad, J. H. Wolter, K. Pierz, M. Roy, and P. A. Maksym, Phys. Rev. B **72**, 165332 (2005).

[20] A. Rastelli, S. Stufler, A. Schliwa, R. Songmuang, C. Manzano, G. Costantini, K. Kern, A. Zrenner, D. Bimberg, and O. G. Schmidt, Phys. Rev. Lett. **92**, 166104 (2004).

[21] A. Rastelli, R. Songmuang, and O. G. Schmidt, Physica E (Amsterdam) **23**, 384 (2004).

[22] S. S. Li, K. Chang, and J. B. Xia, Phys. Rev. B **71**, 155301 (2005).

[23] A. Rastelli, Physica E (to be published).

[24] M. Benyoucef, A. Rastelli, O. G. Schmidt, S. M. Ulrich, and P. Michler (unpublished).

[25] S. N. Walck, T. L. Reinecke, and P. A. Knipp, Phys. Rev. B **56**, 9235 (1997).

[26] N. Schildermans, M. Hayne, V. V. Moshchalkov, A. Rastelli, and O. G. Schmidt, Phys. Rev. B **72**, 115312 (2005).

[27] U. Ekenberg, Phys. Rev. B **40**, 7714 (1989).

[28] Jasprit Singh, *Semiconductor Devices: Basic Principles* (Wiley, New York, 2001).

[29] I. Vurgaftman, J. R. Meyer, and L. R. Ram-Mohan, J. Appl. Phys. **89**, 5815 (2001).

[30] K. Nishibayashi, T. Okuno, Y. Masumoto, and Hong-Wen Ren, Phys. Rev. B **68**, 035333 (2003).